Proc. of the European Safety and Reliability Conference (ESREL 2026)
Edited by José C. Matos, Paulo B. Lourenço, Michael Beer, Daniel Oliveira,
Edoardo Patelli, Hélder S. Sousa, Rui A. Silva and Monica Santamaria
 Published by Research Publishing, Singapore.
doi: 10.3850/ESREL2026061419_esrel26-p26311-cd

Balancing performance and reliability in ammonia-fuelled SOFCs

Lincoln Josue Arellano Ortega
University of Twente, Enschede, The Netherlands. E-mail: l.j.arellanoortega@utwente.nl

Annemieke Angelique Meghoe
University of Twente, Enschede, The Netherlands. E-mail: a.a.meghoe@utwente.nl

Richard Loendersloot
University of Twente, Enschede, The Netherlands. E-mail: r.loendersloot@utwente.nl

Tiedo Tinga
University of Twente, Enschede, The Netherlands & Netherlands Defence Academy, Den Helder, The Netherlands. E-mail: t.tinga@utwente.nl

Ammonia is increasingly positioned as a carbon-free fuel for solid oxide fuel cells (SOFCs). However, direct ammonia feeding can induce nickel nitriding at the anode, accelerating stack degradation. Current work explores some countermeasures, including anti-nitriding coatings, alternative anode materials, and changes in system design. The latter is particularly attractive among these options since system-level redesign can protect the stack and improve efficiency. Accordingly, this paper evaluates the reliability of four SOFC system designs that combine two key measures: anode off-gas recirculation (AOR) to enhance performance, and ammonia pre-cracking to limit nitride formation. The present study integrates Reliability Block Diagrams with Weibull analysis to quantify how each configuration affects overall system reliability and the contribution of critical subsystems. Results indicate that combining AOR with a pre-cracker yields the highest reliability; pre-cracking alone increases reliability but entails an efficiency penalty; and AOR alone, although performance-enhancing, does not provide a reliability justification. To complement these findings, a cost-effectiveness perspective is included to indicate the relative cost implications of moving between configurations. In this way, a balanced view of performance, reliability, and cost is presented. This work therefore provides practical guidance for the design of ammonia-fuelled SOFC systems and supports viable technology selections that extend stack lifetime without compromising system performance.

Keywords: Reliability Block Diagram (RBD), Weibull analysis, solid oxide fuel cell (SOFC), nickel nitriding, reliability assessment.

1. Introduction

Solid oxide fuel cells (SOFCs) are widely recognized for their high electrical efficiency and fuel flexibility. Ammonia is particularly attractive as a carbon-free energy carrier due to its straightforward storage, easier liquefaction, and lower flammability compared to hydrogen (Elmutasim et al., 2024). Consequently, ammonia is increasingly considered a viable option for decarbonizing power generation and marine propulsion systems.

Despite these benefits, durability remains a significant challenge for SOFC technology. This challenge becomes more pronounced when ammonia is used as the primary fuel. In particular, direct ammonia feeding to the anode raises serious concerns related to nickel nitriding. When uncracked ammonia contacts nickel (Ni) particles in the anode (Ni/YSZ cermet), nickel nitride (Ni_3N) is formed (Yang et al., 2015; Rizvandi et al., 2024). This makes the anode less conductive, which reduces the stack's overall performance and the expected stack lifetime (Machaj et al., 2026).

In response to this issue, several mitigation strategies have been investigated at material and operating level. Measures such as increasing operating temperatures (Nemati et al., 2024), or developing anti-nitriding coatings (Curnan et al., 2025) have been explored. These approaches can be effective at cell and stack level. However, they often introduce new trade offs, such as higher degra-

dation rates for other stack materials at elevated temperatures or increased manufacturing costs.

Alternatively, system-level modifications are being explored to protect the stack while optimizing system efficiency. For instance, a detailed efficiency-oriented analysis of ammonia-fueled SOFC systems was conducted by Nemati et al. (2025) using a multiscale modeling approach. In particular, the influence of anode off-gas recirculation (AOR) and external pre-cracking on system performance and nitriding degradation was investigated.

Despite the interplay between these design strategies, a quantitative assessment of their combined effect on system reliability is absent from the literature. This gap is critical for long-life energy systems, particularly in marine applications. Vessels operate for extended periods and require minimal unplanned downtime. Designers therefore require clear insights into how specific design choices influence the risk of premature failure. At the same time, the financial impact of these configurations must be considered, as capital, fuel, and maintenance costs are driven by both efficiency and reliability.

In this work, a step toward this integrated perspective is taken. The reliability of the four ammonia-fueled SOFC system configurations proposed by Nemati et al. (2025) is assessed. By integrating Reliability Block Diagrams with Weibull analysis, this study estimates reliability curves and identifies critical subsystem contributions. Consequently, the main weakness of SOFC systems, limited durability, is addressed in a structured and quantitative manner.

The remainder of this paper is structured as follows: Section 2 details the methodology. Section 3 presents the results of the reliability analysis for the investigated configurations. Section 4 discusses the implications for design optimization and cost-reliability trade-offs. Finally, Section 5 forwards the main conclusions.

2. Methodology

2.1. *Reliability Block Diagram Modeling*

The Reliability Block Diagram (RBD) method is used to describe the logical structure of the system. In this approach, the system is divided into functional blocks that represent its main components. These blocks are arranged in series or parallel to indicate how the system responds to individual component failures (Tinga, 2013).

- **Series configuration:** Failure of any block results in system failure.

$$R_{\text{sys}}(t) = \prod_{i=1}^{n} R_i(t) \tag{1}$$

- **Parallel configuration:** The system remains functional as long as at least one block operates.

$$R_{\text{sys}}(t) = 1 - \prod_{i=1}^{n} [1 - R_i(t)] \tag{2}$$

where R_{sys} is the system reliability and R_i are the reliabilities of individual blocks.

2.2. *Weibull Distribution*

To characterize the time-dependent reliability of each component, the two-parameter Weibull distribution is employed:

$$R_i(t) = e^{-(t/\eta)^{\beta}} \tag{3}$$

The Weibull distribution is used to represent different failure behaviors and predicting component lifetime. It is defined by two parameters: the shape parameter (β) and the scale parameter (η). The shape parameter β determines how the failure rate evolves with time. When $\beta < 1$, failures occur predominantly in the early life of the component. A value of $\beta = 1$ indicates a constant failure rate, typical of random failures. Conversely, $\beta > 1$ reflects a wear-out phase, where the failure rate increases as the component ages. The scale parameter η, also known as the characteristic life, denotes the time at which approximately 63.2% of a population is expected to fail. Larger values of η indicate longer expected lifetimes.

Weibull parameters values are typically obtained from historical failure data. However, for the present case study, data for SOFC systems operating with ammonia are scarce due to the emerging nature of this technology. Consequently, the dominant failure mechanisms of each component are identified and used to establish representative Weibull parameters. These parameters are

assigned based on the physical characteristics of each failure mode, as discussed in Section 3.

2.3. *Cost-effectiveness analysis*

In this analysis, three cost elements are evaluated: annualised Capital Expenditure (CAPEX), fuel, and Operation and Maintenance (O&M) costs. Capital costs are derived using the Capital Recovery Factor (CRF), assuming an interest rate (i) of 5% and a system lifetime (n) of 20 years:

$$\mathrm{CRF} = \frac{i(1+i)^n}{(1+i)^n - 1} \tag{4}$$

$$C_{\text{Ann. CAPEX},k} = \mathrm{CAPEX}_k \cdot \mathrm{CRF} \tag{5}$$

Fuel costs are estimated from the delivered electrical energy (E_{elec}) and efficiency (η_{elec}), as follows:

$$C_{\text{fuel},k} = \dot{m}_{\mathrm{NH_3},k} \cdot P_{\mathrm{NH_3}} \tag{6}$$

where $P_{\mathrm{NH_3}}$ is the market price of ammonia, and the mass flow rate $\dot{m}_{\mathrm{NH_3}}$ is determined by:

$$\dot{m}_{\mathrm{NH_3}} = \frac{E_{\text{elec}}}{\eta_{\text{elec}} \cdot \mathrm{LHV}_{\mathrm{NH_3}}} \tag{7}$$

Routine O&M costs are estimated by linking the cost rate to the system's robustness. The reference annual O&M rate is taken as 5.5% of the total CAPEX for Configuration 1 (Liu et al., 2025). For the alternative configurations, the output of the reliability assessment is used as follows:

$$\mathrm{O\&M}_{\text{rate},k} = 0.055 \cdot \frac{t_{50,C_1}}{t_{50,C_k}} \tag{8}$$

In this expression, t_{50,C_k} denotes the time at which the reliability of configuration k reaches $R(t) = 0.5$. Through this formulation, more reliable systems are associated with lower O&M rates, reflecting the expectation of fewer failures and less frequent corrective maintenance.

The total annual cost is subsequently obtained by summing these three indicators:

$$C_{\text{annual},k} = C_{\text{Ann. CAPEX},k} + C_{\text{fuel},k} + C_{\text{O\&M},k} \tag{9}$$

To conclude this assessment, the Levelised Cost of Energy (LCOE) is calculated as:

$$\mathrm{LCOE}_k = \frac{C_{\text{annual},k}}{E_{\text{elec}}} \tag{10}$$

3. Results and Discussion

3.1. *System Definition*

The four system configurations are presented in Fig. 1. The dotted gray region outlines the baseline system components common to all designs, while the optional subsystems are grouped into color-coded subsystems. The configurations are defined as follows:

- **Configuration 1:** Baseline system (gray area) without pre-cracking or AOR.
- **Configuration 2:** System with the pre-cracking unit (yellow area) only.
- **Configuration 3:** System with the AOR loop (purple area) only.
- **Configuration 4:** System combining both pre-cracking (yellow area) and AOR (purple area).

These configurations are then represented using RBDs, as shown in Fig. 2. For the reliability results, the system is also described in terms of functional subsystems, and the labels used in the reliability plots refer to the following component groupings: *Air supply* = compressor 1; *Thermal management* = $\mathrm{HE_1}$, $\mathrm{HE_2}$, ($\mathrm{HE_3}$), $\mathrm{HE_4}$; *Fuel from storage* = $\mathrm{NH_3}$, tank, ($\mathrm{HE_3}$); *Fuel from recirculation* = condenser, compressor 2; and *Cracking* = bypass, cracker.

3.2. *Failure Analysis*

This section examines the degradation pathways of the SOFC system. The assigned representative Weibull parameters are summarized in Table 1.

3.2.1. *High-Temperature Components*

SOFC stack: Stack degradation is heavily influenced by the fuel processing strategy. Systems utilizing a pre-cracking unit convert ammonia to hydrogen prior to stack entry; consequently, failure is governed by *nickel particle coarsening*, mimicking hydrogen-fueled systems (Chang et al., 2025). Conversely, direct ammonia feeding promotes *nickel nitriding*, which accelerates long-term degradation (Nemati et al., 2024). Both mechanisms exhibit wear-out behavior ($\beta = 3.0$). Modern SOFC stacks demonstrate continuous op-

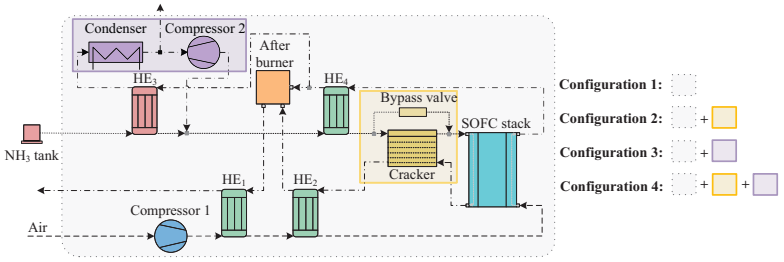

Fig. 1. Unified schematic illustrating the modular architecture of the four system configurations.

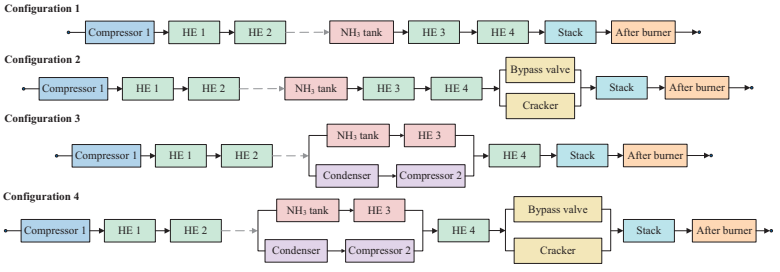

Fig. 2. Reliability Block Diagrams (RBDs) of the four SOFC configurations. The color coding follows the modular architecture defined in Fig. 1.

eration for around five years, supporting a characteristic life of $\eta = 40\,\text{kh}$ under pre-cracked fuel conditions (Mehran et al., 2023). For systems operating directly on ammonia, a reduced life of $\eta = 15\,\text{kh}$ is assumed.

Heat exchanger: This component faces corrosion of the catalyst on the fuel side and fouling on the air side (Ali et al., 2020). Both affect heat transfer and induce local overheating. Consistent with high-temperature heat exchangers, a shape factor of $\beta = 2.75$ and a characteristic life of $\eta = 40\,\text{kh}$ are assumed, reflecting design intents for long service intervals (Åström et al., 2007).

After burner: The post-burner combusts any residual fuel from the SOFC anode exhaust with air, generating additional heat and ensuring complete fuel utilization. The burner itself is less affected by these by-products than downstream components; however, its metallic parts operate in a high-temperature, which promotes thermal fatigue and oxidation. A shape factor of $\beta = 2.5$ and a characteristic life of $\eta = 40\,\text{kh}$ are selected to represent typical multi-year service capabilities.

Cracker: Ammonia decomposition relies on catalytic activity that naturally diminishes over time. This gradual deactivation dictates a wear-out regime ($\beta = 2.0$). Based on available long-duration tests, a characteristic life of $\eta = 20\,\text{kh}$ is used, reflecting the shorter lifetime compared to the other components (Zhang et al., 2023).

3.2.2. *Balance-of-Plant Components*

Fuel tank: The failure of this component is primarily driven by fatigue from pressure cycling. Reliability is high in early life, slowly transitioning to wear-out ($\beta = 1.1$). As pressure vessels are engineered for service lives exceeding 15-20 years, a characteristic life of $\eta = 150\,\text{kh}$ is assigned (Kostidi and Lyridis, 2025).

Compressor 1: Degradation of this rotating machinery is dominated by mechanical wear, including bearing wear and impeller fatigue. Accordingly, a shape factor of $\beta = 2.75$ is utilized. Comparable compressors indicate long operating

lifetimes, hence a characteristic life of $\eta = 50\,\text{kh}$ is assumed (Åström et al., 2007).

Condenser: The condenser is exposed to moist exhaust gas, which contains traces of ammonia. This induces corrosion and fouling, justifying a wear-out shape factor of $\beta = 2.0$. A characteristic life of $\eta = 60\,\text{kh}$ is estimated, assuming operation is limited by corrosion rates and supplemented by routine maintenance.

Compressor 2: The recirculation compressor operates in a harsher environment than the air compressor, handling hot, humid anode exhaust. While failure modes remain similar to other rotating machinery ($\beta = 2.75$), the accelerated corrosion and wear result in a reduced life of $\eta = 30\,\text{kh}$.

Table 1. Weibull parameters for the SOFC system.

Component	Key Degradation Mechanisms	β (-)	η (kh)
SOFC stack	Nickel coarsening	3.0	40
	Nickel nitriding	3.0	15
Heat exchanger	Corrosion, fouling	2.75	40
After burner	Thermal fatigue	2.5	40
Cracker	Catalyst deactivation	2.0	20
Fuel tank	Fatigue (cycles)	1.1	150
Compressor 1	Wearing	2.75	50
Condenser	Corrosion, fouling	2.0	60
Compressor 2	Wearing, corrosion	2.75	30

3.3. *Reliability Plots*

Based on the RBD structures defined in Fig. 2 and the Weibull parameters summarized in Table 1, reliability curves are generated for each configuration, as displayed in Fig. 3. These results follow the functional groupings defined in Section 3.1.

3.3.1. *Configuration 1*

Configuration 1 (C1) represents the simplest architecture, with no pre-cracking or recirculation loop included. As illustrated in Fig. 3a, the reliability of the stack is observed to decrease significantly faster than that of the supporting subsystems. This rapid decline is attributed to the direct feeding of ammonia, which induces nickel nitridation and accelerates anode degradation compared to hydrogen-fuelled operations. Since the balance-of-plant components are in good condition over the assessment period, the stack is identified as the dominant reliability bottleneck. Consequently, the necessity for mitigation strategies to protect the anode becomes the primary driver for the alternative designs discussed below.

3.3.2. *Configuration 2*

To mitigate the accelerated stack degradation identified in C1, C2 introduces an external cracker unit and a bypass valve. This design modification allows the stack to be supplied primarily with hydrogen, thereby altering the degradation physics. As the lifetime depends on the cracking percentage x, the effective characteristic life is derived via a linear interpolation of the failure-rate parameters:

$$\eta_{stack}(x) = \left[(1-x)\eta_{\text{nitrid}}^{-\beta} + x\eta_{\text{coars}}^{-\beta}\right]^{-\frac{1}{\beta}} \quad (11)$$

This formulation is applied assuming a cracking rate of $x = 0.9$ (Nemati et al., 2025). Fig. 3b shows that the decline in stack reliability is slowed compared to C1, confirming the benefit of cracking ammonia prior to the anode. Although degradation is shifted from the stack to the cracking unit, the fuel-processing subsystem includes a parallel configuration of the cracker and bypass valve operating as a back-up. This is why the overall system reliability remains relatively high.

3.3.3. *Configuration 3*

In contrast to the protective strategy of pre-cracking, C3 is designed to enhance performance by integrating an AOR loop while maintaining direct ammonia feeding to the stack. Fig. 3c reveals that this configuration exhibits the steepest degradation curve among all analyzed designs. This deterioration is explained by the increased flow rates associated with recirculation; the residence time of ammonia at the catalyst surface is reduced, allowing a higher fraction of uncracked ammonia to reach the anode and exacerbating the formation of nickel nitrides. While this configuration is reported to yield the highest system efficiency, its long-term reliability is found to be

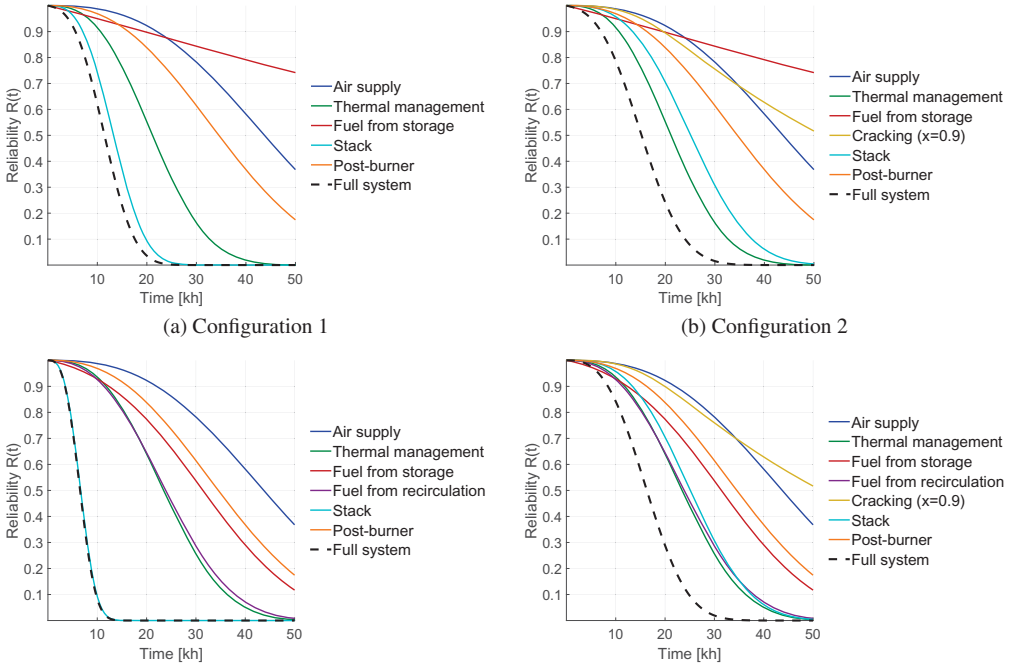

(a) Configuration 1 (b) Configuration 2

(c) Configuration 3 (d) Configuration 4

Fig. 3. Reliability curves for the analyzed configurations.

severely compromised. It is therefore concluded that without pre-cracking, the efficiency gains of AOR are negated by premature stack failure.

3.3.4. *Configuration 4*

Building upon the insights gained from the previous configurations, C4 is designed to combine the protective benefits of pre-cracking with the efficiency gains of AOR. As shown in Fig. 3d, the stack reliability curve is significantly higher than in C1 and C3, a result of the hydrogen operation. Furthermore, the accelerated degradation observed in C3 is successfully neutralized, as the high recirculation flow no longer carries uncracked ammonia to the anode. This shows that by coupling these technologies, the failure trend is shifted away from the critical stack component, offering a more resilient system architecture.

3.4. *Overall reliability*

By comparing the dashed lines in Fig. 3, it is confirmed that C4 balances the operational longevity required for typical marine applications with the performance requirements. While C3 was previously identified as the most efficient, its poor reliability metrics render it operationally unfeasible for long-term deployment. Consequently, C4 is recommended as the preferred design choice, as it successfully extends stack lifetime without the severe penalties associated with direct ammonia feeding. The economic implications of transitioning between configurations remain an open question and are examined in the following section.

3.5. *Cost-effectiveness Analysis*

The financial implications of adopting the four SOFC configurations are evaluated in this section, providing a general perspective on the most influential cost drivers.

3.5.1. *Assumptions and Boundary Conditions*

The assessment is carried out for a 700 kW ammonia-fuelled SOFC system operating 6000 h per year over a 20-year vessel lifetime, which

is a typical marine deployment. Under these conditions, the annual electricity production is $E_{\text{elec}} = 4200\,\text{MWh}$.

3.5.2. *Total costs*

First, the capital cost contribution is considered. C1 represents the simplest plant architecture, with a stack and base balance-of-plant cost of approximately $\$2000/\text{kW}$ (Liu et al., 2025). Introducing an external cracker in C2 increases the specific CAPEX by $\$500/\text{kW}$, whereas the AOR loop in C3 adds around $\$300/\text{kW}$. C4, which combines both technologies, therefore becomes the most capital-intensive system, with a total of $\$2800/\text{kW}$. These values are used in Eq. (5) to compute the corresponding annualised CAPEX.

Next, the fuel cost is determined. The ammonia mass flow rate is calculated from Eq. (7) using the electrical efficiency (η_{elec}) reported in Table 3. The lower heating value of ammonia is taken as $\text{LHV}_{\text{NH}_3} = 18.6\,\text{MJ/kg}$, and a fuel price of $\$500/\text{t}$ is assumed. Under these assumptions, the baseline and pre-cracked systems (C1 and C2) exhibit similar electrical efficiencies and therefore require approximately $1530\text{-}1580\,\text{t}\,\text{NH}_3/\text{yr}$. In contrast, the configurations with AOR (C3 and C4) achieve substantially higher efficiencies, reducing annual fuel demand to about $1080\text{-}1130\,\text{t}\,\text{NH}_3/\text{yr}$ and thus proportionally lowering the annual fuel cost. This step explicitly shows that operational efficiency is a major driver of the total lifecycle expenditure.

Finally, the O&M costs are estimate by utilizing Eq. (8) to correlate the cost rate with system reliability. The resulting annualised CAPEX, fuel costs, O&M costs, total annual costs, and LCOE are summarised in Table 2. For comparison purposes, the most relevant metrics are summarized in Table 3.

C1, despite having a moderate capital cost, is burdened by the high fuel consumption associated with its lower efficiency, resulting in an LCOE of $\$0.227/\text{kWh}$. C2, which includes the cracker but lacks AOR, exhibits a cost increase without a corresponding improvement in efficiency. Consequently, the highest LCOE ($\$0.238/\text{kWh}$) is observed for this design. In sharp contrast, C3 achieves a lower LCOE ($\$0.197/\text{kWh}$), which is driven primarily by its high efficiency and the resulting reduction in fuel consumption. However, this configuration was previously identified as the least reliable option, since direct ammonia supply accelerates stack degradation.

Table 2. Cost overview of the SOFC configurations.

	Power (kW)	CAPEX ($/kW)	Fuel cost (k$/yr)	O&M cost (k$/yr)	Total cost (k$/yr)	LCOE ($/kWh)
C1	700	112.3	765.4	5.5% of the CAPEX	954.8	0.227
C2	700	140.4	787.7	4.2% of the CAPEX	1000.6	0.238
C3	700	129.2	542.7	9.7% of the CAPEX	827.3	0.197
C4	700	157.3	564.5	3.9% of the CAPEX	797.5	0.190

Table 3. Performance and reliability metrics.

Config.	Efficiency (%)	Reliability (kh)	LCOE ($/kWh)
C1	53.1	11.45	0.227
C2	51.6	15.20	0.238
C3	74.9	6.52	0.197
C4	72.0	16.30	0.190

Source: Efficiency reported by Nemati et al. (2025) and reliability metrics taken at $R(t) = 0.5$.

Therefore, C4 is found to yield the most balanced outcome. Although its capital cost is the highest, the combination of improved efficiency and extended stack lifetime limits its operating expenses. This synthesis results in the most competitive LCOE ($\$0.190/\text{kWh}$), while simultaneously offering the superior reliability performance among all configurations. This combination of technical and economic advantages supports the selection of C4 as the most favorable design when lifetime performance and operational robustness are considered together.

4. Conclusion

This study establishes a critical balance between performance, reliability, and cost-effectiveness for ammonia-fuelled SOFC systems. The comparative assessment identifies the combined configu-

ration of pre-cracking and anode off-gas recirculation (C4) as the optimal design, since it delivers the lowest LCOE and improved system longevity by mitigating nickel nitriding. By contrast, the configuration utilizing recirculation only (C3) is deemed unsuitable for long-term operation due to poor reliability, despite its high efficiency; meanwhile, the pre-cracking-only approach (C2) enhances durability at the expense of higher cost. Beyond these findings, this work highlights the value of evaluating system performance over the expected operational lifetime to support designers, ship owners, and policy makers in addressing barriers to the adoption of SOFC technology. The quantitative values reported here are based on estimated Weibull parameters and should be updated when failure data become available; however, the relative trends identified in this work are expected to remain valid. Furthermore, the assumed effect of improved reliability on reducing maintenance costs may be different for other applications.

Acknowledgement

This research is supported by the AmmoniaDrive project (project 14267) which is financed by the Netherlands Organisation for Scientific Research (NWO).

References

Ali, M., A. Ul-Hamid, L. M. Alhems, and A. Saeed (2020). Review of common failures in heat exchangers – Part I: Mechanical and elevated temperature failures. *Engineering Failure Analysis 109*, 104396.

Chang, J., P. Zhang, Y. Sun, Q. Wang, Z. Yang, and H. Zeng (2025). Temperature-driven degradation in SOFCs: Insights into anode microstructure evolution and Ni agglomeration. *International Journal of Hydrogen Energy 102*, 1421–1431.

Curnan, M. T., K. C. Min, J. H. Shim, and G. H. Gu (2025). Elucidating conductivity and nitriding resiliency in (Al/H)-ZnO coatings for NH3-fueled SOFC separators via SEM-EDX and MLP-DFT protocols. *Journal of Materials Chemistry A 13*(22), 16728–16739.

Elmutasim, O., S. Giddey, D. S. Dhawale, and S. Bhattacharya (2024). Ammonia to power: Advancing direct ammonia SOFCs through experimental and theoretical studies. *International Journal of Hydrogen Energy 96*, 192–209.

Kostidi, E. and D. Lyridis (2025). Customizable Life Cycle Cost Methodology for Ammonia Fuel Storage: Enhancing Adoptability Across Diverse Onboard Arrangements. *Energies 18*(5), 1228.

Liu, Y., M. Luo, W. Li, C. Zhou, X. Huo, Z. Pan, R. Chen, and L. An (2025). Techno-economic analysis of using ammonia as an energy carrier for renewable energy conversion and storage. *International Journal of Hydrogen Energy 162*, 150784.

Machaj, K., Y. Naumovich, M. Kosiorek, L. Ajdys, A. Niemczyk, P. Ostrowski, M. Łazor, M. Wierzbicki, A. Koprowska, M. Skrzypkiewicz, and M. Skrzypkiewicz (2026). Studies of ammonia-fueled SOFC stacks: Insights into possible failure causes. *Fuel 405*, 136579.

Mehran, M. T., M. Z. Khan, R.-H. Song, T.-H. Lim, M. Naqvi, R. Raza, B. Zhu, and M. B. Hanif (2023). A comprehensive review on durability improvement of SOFCS for commercial stationary power generation systems. *Applied Energy 352*, 121864.

Nemati, A., H. Nami, J. Beyrami, R. N. Nakashima, and H. L. Frandsen (2025). Efficient and durable system design for ammonia-fueled SOFCs using multiscale multiphysics modeling approach. *Fuel 392*, 134837.

Nemati, A., O. B. Rizvandi, F. Mondi, and H. L. Frandsen (2024). Detailed 3D multiphysics modeling of an ammonia-fueled SOFC: Anode off-gas recirculation and Ni nitriding degradation. *Energy Conversion and Management 308*.

Nemati, A., O. B. Rizvandi, R. N. Nakashima, J. Beyrami, and H. L. Frandsen (2024). Multiscale multiphysics modeling of ammonia-fueled SOFC: Effects of temperature and pre-cracking on reliability and performance of stack and system. *Applied Energy 373*, 123913.

Rizvandi, O. B., A. Nemati, M. Chen, and H. L. Frandsen (2024). A numerical investigation of nitridation in SOFC stacks operated with ammonia. *International Journal of Hydrogen Energy 50*, 961–976.

Tinga, T. (2013). Principles of loads and failure mechanisms. *Springer Series in Reliability Engineering*.

Yang, J., A. F. S. Molouk, T. Okanishi, H. Muroyama, T. Matsui, and K. Eguchi (2015). A Stability Study of Ni/Yttria-Stabilized Zirconia Anode for Direct Ammonia SOFCs. *ACS Applied Materials & Interfaces 7*(51), 28701–28707. doi: 10.1021/acsami.5b11122.

Zhang, Y., N. Zhao, M. Li, Z. Xu, D. Wu, S. Hillmansen, A. Tsolakis, K. Blacktop, and C. Roberts (2023). A techno-economic analysis of ammonia-fuelled powertrain systems for rail freight. *Transportation Research Part D: Transport and Environment 119*, 103739.

Åström, K., E. Fontell, and S. Virtanen (2007). Reliability analysis and initial requirements for FC systems and stacks. *Journal of Power Sources 171*(1), 46–54.